NASA Technical Memorandum 78635

Influence of Free-Stream Disturbances on Boundary-Layer Transition

William D. Harvey

APRIL 1978

NASA

NASA Technical Memorandum 78635

Influence of Free-Stream Disturbances on Boundary-Layer Transition

William D. Harvey
Langley Research Center
Hampton, Virginia

National Aeronautics
and Space Administration

**Scientific and Technical
Information Office**

1978

SUMMARY

Considerable experimental evidence exists which shows that free-stream disturbances (the ratio of root-mean-square pressure fluctuations to mean values) in conventional wind tunnels increase with increasing Mach number at low supersonic to moderate hypersonic speeds. In addition to local conditions, the free-stream disturbance level influences transition behavior on simple test models. Based on this observation, existing noise-transition data obtained in the same test facility have been correlated for a large number of reference sharp cones and flat plates and are shown to collapse along a single curve. This result is a significant improvement over previous attempts to correlate noise-transition data.

INTRODUCTION

The difficulty of reconciling large differences in transition measurements on simple bodies in different wind tunnels, as well as differences in tunnel measurements and flight measurements, is well-known. Many factors influence transition, and unit Reynolds number and wind-tunnel disturbance-level effects are among the least consistent and least understood. Aeroballistic ranges and the flight environment are essentially disturbance free, and unit Reynolds number effects that are somewhat different from those observed in wind tunnels with inherent free-stream disturbances have been found in both cases (refs. 1 and 2). A revealing evaluation of the many factors (which can combine in complex ways) that affect transition has been extensively described in references 3 to 5. Numerous researchers (refs. 6 to 13) have established that transition in supersonic wind tunnels is influenced by free-stream acoustic disturbances that are radiated from the turbulent boundary layers on the tunnel walls. Detailed amplitude and frequency composition of these disturbances is generally peculiar to a particular tunnel; therefore, Reynolds number scaling can be influenced to various degrees. In general, pressure fluctuations are the dominant free-stream disturbance mode that affects unsteady aerodynamic tests in transonic wind tunnels and boundary-layer stability in high supersonic/hypersonic wind tunnels. Turbulent boundary layers radiate sound with increasing efficiency as the free-stream Mach number M_∞ is increased because radiation sources acquire relative supersonic phase velocities, and the overall intensity of the sound is Reynolds number dependent. Reference 14 has shown that, in the JPL 20-Inch Supersonic Wind Tunnel, the radiated intensity from the turbulent boundary layer scales with the square of the wall shear stress and is about 1/5 to 1/4 of the shear stress measured on the tunnel wall for supersonic flow ($1.5 \leq M \leq 5$). If the pressure fluctuations are nondimensionalized by the mean shear stress at the wall, the Reynolds number effect disappears and the radiated field scales with this boundary-layer parameter (ref. 14).

This paper is concerned with a simplified correlation of wind-tunnel disturbances with transition on simple models (cones and flat plates) by using

free-stream disturbance levels available from either hot-wire anemometer data or acoustic pressure transducers that are mounted flush with the surface of the cones and flat plates beneath laminar boundary layers. Earlier attempts (refs. 6 to 8, 15, and 16) to relate transition Reynolds number with nondimensional free-stream pressure fluctuations were unsuccessful in collapsing results for several facilities and Mach numbers. References 13, 17, and 18 correlated transition Reynolds numbers for a large number of wind tunnels at $2 \leq M_\infty \leq 8$ based on parameters such as local conditions at the tunnel wall, tunnel size, and radiated sound. Reference 19 correlated wind-tunnel noise data with reasonable success over a range of Mach numbers and tunnel size: for supersonic/hypersonic flow in terms of free-stream and local parameters. Free-stream disturbance levels and transition measurements in a large number of wind tunnels have recently been compared (ref. 20), and although no clear understanding of the mechanisms influencing the transition process was revealed, no doubt remains that transition is influenced by free-stream disturbances over the entire speed range.

This paper also attempts to extend earlier results by comparing the variations in wall and stream disturbances over a wide range of Mach number and Reynolds number in wind tunnels of different sizes.

SYMBOLS

f	frequency
M	Mach number
p	mean static pressure
q	dynamic pressure, $\frac{\gamma}{2} pM^2$
R	unit Reynolds number
rms	root mean square
t	temperature
U	velocity
α	angle of attack
τ	shear stress
γ	ratio of specific heats
θ_c	cone half-angle

Subscripts:

a	based on acoustic origin

e	edge conditions
l	local conditions
t	total conditions
tr	transition
w	wall conditions
∞	free stream
'	fluctuating values

WALL AND FREE-STREAM PRESSURE FLUCTUATIONS

The measurement difficulties and final data accuracy of individual referenceable results are rarely reported. Therefore, data accuracy is difficult to identify and is too numerous and complicated to evaluate properly in this paper. However, sufficient data are available to establish the general level and trend of wind-tunnel noise for a rather wide range of test conditions, as shown in figure 1. (See table I for data source and refs. 2, 7 to 9, 13 to 18, and 21 to 29.) The free-stream rms pressure fluctuations have been divided by the mean static pressure (fig. 1(a)) and by the dynamic pressure (fig. 1(b)) in order to compare the variation of radiated sound with and without free-stream Mach number effects. These data have been obtained by either hot-wire anemometry or pressure transducers that have been mounted flush with the surface of sharp cones and flat plates beneath laminar boundary layers (except for the electron-beam rms density results (discussed in ref. 21 and shown in fig. 1 as cross-circles at $M_\infty = 20$) in which rms density and pressure fluctuations have been assumed proportional (ref. 14), that is, negligible vorticity).

It has previously been shown that the acoustic pressure (p'/p) is not greatly changed after passing through weak oblique shocks (refs. 15 and 19). Therefore, surface acoustic measurements are considered to be an adequate representation of free-stream disturbance intensity levels. All values of M_∞ for helium in figure 1 (data source given in table I) have been corrected to equivalent values of M_∞ for air by using the equation $M_{\infty,air} = 1.291 M_{\infty,He}$ which is based on $(\gamma - 1)M^2 = \text{Constant}$. (See ref. 30.) The solid symbols (fig. 1) are for data from transonic tunnels with either perforated or slotted walls. It has been experimentally shown that $\sqrt{\overline{p_\infty'^2}}/p_\infty$ generally decreases with increasing unit Reynolds number for a given supersonic/hypersonic wind tunnel and increases with test Mach number when the wall boundary layer is turbulent (refs. 6, 7, and 9). Therefore, the observed variation in disturbance level (fig. 1) for a given M_∞ is mainly due to a unit Reynolds number effect. It should be noted that all the reference disturbance data presented in figure 1 are plotted against M_∞ at the sensor axial location in their respective tunnel test section except for the unpublished data obtained in the Mach 5 pilot quiet tunnel at the Langley Research Center and the published results (ref. 24) obtained in the same tunnel. These latter results have been plotted against

the upstream acoustic origin Mach numbers ($2.27 \leq M_a \leq 5$) that correspond to several axial probe locations within the flow test rhombus by tracing along characteristic lines calculated for the rapid-expansion Mach 5 pilot quiet tunnel at the Langley Research Center (ref. 24). These data demonstrate the interesting result that disturbances can decrease to very low levels in the upstream end of the test rhombus of this nozzle ($M_a = 2.27$) and can approach close agreement with disturbance levels from conventional tunnels that have more gradual expansions and with corresponding values of M_∞. The disturbance level in two different nozzle geometries with $M_\infty = 2.3$ (fig. 1) was measured and is reported in reference 29. A higher level was obtained in the two-dimensional half nozzle with one flat side wall than in a symmetric nozzle; this fact suggested that favorable pressure gradients may be important in reducing disturbances. Relative to the zero-pressure gradient case, the ratio of rms wall pressure fluctuations to dynamic pressure fluctuations is greater in an adverse gradient than in a favorable gradient. Further studies are required to determine whether these new results are due to the large favorable pressure gradients in the rapid-expansion nozzle, to reduced energy at low-frequency geometry, or simply to a reduction in noise level that is caused by the decreasing boundary-layer thickness and Mach number as the throat is approached.

Figure 1(a) clearly shows that acoustic disturbances in transonic tunnels increase rapidly with Mach number at $0.2 < M_\infty < 1.0$. These results can be affected by diffuser design, tunnel-wall—hole resonance, flow through slotted walls, model support, and fan noise. It is generally found that acoustic resonance effects in transonic tunnels with open slots have characteristic frequencies less than about 200 Hz. The disturbance levels for $1.5 \leq M_\infty \leq 2$ in supersonic tunnels are considerably lower than for transonic tunnels (fig. 1). However, values of $\sqrt{\overline{p'^2}}/p_\infty$ again increase with increasing Mach number (fig. 1(a)) although they have a tendency to level off or possibly decrease at high hypersonic speeds ($M_\infty \geq 20$) and are dominated by radiation from the turbulent boundary layer on the wall (refs. 6 to 13).

The tentative data fairings in figure 1 are intended to represent an average trend without considering unit Reynolds number effects. It should also be noted that there appears to be no significant effect of wall cooling on disturbance level, at least for the limited results shown.

Radiated pressure fluctuations divided by either free-stream local static pressure (fig. 1(a)) or dynamic pressure (fig. 1(b)) exhibit a wide scatter, mainly because of unit Reynolds number effects. The data and predictions (refs. 16 and 31) presented in figure 2 (see table II for data source and refs. 6 to 8, 13 to 16, 21 to 23, 25, 26, and 32 to 42) include the effects of unit Reynolds number (refs. 14 and 32) and Mach number by dividing the rms pressure fluctuations measured either at the tunnel wall or in the free stream by the test-section local wall shear stress. Except for the electron-beam results of reference 21, the free-stream data (solid symbols) have been obtained by either hot-wire anemometry or acoustical transducers on models beneath laminar boundary layers. The wall data (open symbols) have been obtained either with acoustic transducers beneath a turbulent boundary layer on the tunnel wall or under turbulent boundary layers on flat plates (refs. 40 and 41) in the free

stream and were considered equivalent. All values of M_∞ for helium have been corrected to values of M_∞ for air (ref. 30).

With the exception of data obtained on the flat plates (refs. 39 and 41), the general trend for wall data (fig. 2) is to gradually increase in level for $0.1 < M_\infty < 10$, with an indication of leveling off at high speeds. The wall predictions in reference 31 and the free-stream predictions in reference 16 agree with the general trend of the data that are mainly for adiabatic conditions (table II). For the limiting values of $M_\infty = 0$ and ∞, the respective normalized disturbances based on the present data fairings are $\sqrt{p_w'^2}/\tau_w = 2.5$ and 5.3. Utilizing these limiting values and an approach similar to that applied earlier (ref. 19), the following relation may be used for the wall data and $t_w/t_t = 1.0$ (shown in fig. 2):

$$\frac{\sqrt{p_w'^2}}{\tau_w} = 2.5 + 2.8\left(1 - e^{-0.1M_\infty^2}\right) \tag{1}$$

Except for the data of reference 13 which seem excessively high for currently unknown reasons, the free-stream data represented by the present fairing are considerably lower in magnitude than the wall data at low speeds but increase with Mach number to an apparent peak at $8 < M_\infty < 10$ (fig. 2). Surprisingly, above about $M_\infty \approx 10$, $\sqrt{p_\infty'^2}/\tau_w$ decreases with increasing M_∞, perhaps due to the lower t_w/t_t values for many of these high Mach number results.

The results shown in figures 1 and 2 clearly indicate that inherent disturbance levels in most ground-based test facilities are much higher than the low level anticipated for flight-simulation and natural-transition studies (refs. 2, 43, and 44). However, if the data presented in figures 1 and 2 and reference 19 can be accepted as representative of the disturbance levels in conventional wind tunnels, then estimates of either the wall or free-stream pressure fluctuations can be made for any wind tunnel. For example, the free-stream pressure fluctuations in available supersonic wind tunnels may be estimated from the following equation:

$$\frac{\sqrt{p_\infty'^2}}{p_\infty} \propto R_\infty^{-0.3M_\infty^2} \qquad (1.5 < M_\infty < 10) \tag{2}$$

where R_∞ is the free-stream unit Reynolds number and the constant of proportionality is presumably a function of tunnel geometry. Equation (2) is not applicable over the subsonic and transonic speed range. In general, the wind-tunnel free-stream rms pressure fluctuations divided by the mean static pressure can be expected to increase with increasing speed ($1.5 \lesssim M_\infty \lesssim 10$) at the same unit Reynolds number up to $M_\infty \approx 10$ and then to decrease for $M_\infty \lesssim 20$. For M_∞ less than 1.5, model support and diffuser generated disturbances can cause sound propagation upstream in the test section resulting in the relatively high rms pressure fluctuations in transonic tunnels (fig. 1). Presumably, choking the flow ahead of the support and diffuser in these tunnels would significantly reduce the stream disturbance level.

CORRELATION OF TRANSITION REYNOLDS NUMBER WITH FREE-STREAM DISTURBANCE LEVEL

Considerable theoretical and experimental evidence exists which suggests that the transition process on models is a function of both local conditions and free-stream disturbance level. Thus, transition results for cones over the speed range are not generally expected to agree with results for flat plates and cylinders at $\alpha = 0^\circ$ (ref. 45). The effect of local Mach number on the beginning of transition was evaluated by comparing values of $R_{1,tr}$ obtained on sharp cones, $2.87^\circ \leq \theta_c \leq 16.75^\circ$, in test facilities of several sizes for a nearly constant value of free-stream disturbance level. These data are shown in figure 3 for typical values of $\sqrt{\overline{p'^2_\infty}}/p_\infty$ found in the ground test facilities and are compared with transition data on cones in flight (ref. 46) and aeroballistic ranges (ref. 1) where stream disturbance levels are considered negligible. The dashed lines in figure 3 are data fairings for nearly constant values of $\sqrt{\overline{p'^2_\infty}}/p_\infty$. All data shown (fig. 3) have unit Reynolds number effects. For example, a bar is used to indicate the spread in $R_{1,tr}$ for the range data (ref. 1). The tunnel data in figure 3 clearly demonstrate a varying effect of local Mach number on transition in the low Mach number region ($M_e < 5$) for a given free-stream disturbance level compared with a much stronger effect in the higher Mach number region ($5 \leq M_e \leq 16$), as shown in reference 9. It appears that for essentially disturbance-free flows and smooth models, transition is mainly a function of local Mach number and unit Reynolds number and $R_{1,tr}$ is expected to increase with increasing M_e.

References 47 and 53 have shown that transition data on sharp cones can be satisfactorily correlated for $3 \leq M_\infty \leq 21$ in several tunnels of varying sizes based on a noise-transition empirical equation. This correlation for the end of transition is a function of tunnel test-section mean skin-friction coefficient, turbulent boundary-layer displacement thickness, test-section circumference, and reference tunnel test-section perimeter. The present attempt to correlate transition data is of course not completely new and stems from the basic premise that the stability of a laminar boundary layer on a model is affected by input disturbance level and local dynamic pressure. Although no direct account is taken of the energy spectra, there is an implicit inclusion of this effect in that the spectra from the various facilities are quite similar. The fact that transition was shown in figure 3 to be a strong function of both free-stream disturbance level and M_e also lends support to the noise parameter used herein. The influence of free-stream disturbance level on transition for cones and flat plates is shown in figures 4 and 5 and may correspond to mode 1 and mode 2 instabilities, respectively, in accordance with results from Mack's linear stability theory (refs. 48 to 50).

Figures 4 and 5 present data for the beginning of transition as a function of either free-stream turbulence level or rms pressure fluctuations divided by local conditions on sharp cones, cylinders, and flat plates at $\alpha = 0^\circ$. The transition data represent a wide range of experiments and conditions (see table III for data source and measurement technique and refs. 1, 6, 7, 9, 10 to 13, 16, 18, 46, and 51 to 61) where both $R_{1,tr}$ and free-stream disturbance

levels were measured in the same facility for a given test model and geometry. Based on profiles of transition for several unit Reynolds numbers of these reference data, data for the end of transition have been adjusted to the beginning of transition by a constant factor of 1.55 for references 11, 13, 17, and 18 and by a factor of 1.33 for reference 10; these data are included in figures 4 and 5.

Figure 4 shows the variation of $R_{1,tr}$ with free-stream disturbance level for $0 \leq M_\infty \leq 4$ where noise-transition dominance could be influenced by mode 1 instabilities (refs. 48 to 50). Transition $R_{1,tr}$ in wind tunnels increases with decreasing disturbance level as expected but approaches differing levels of nearly constant $R_{1,tr}$ at low disturbance levels (less than 10^3) due to characteristic frequencies and wave orientation in the disturbance spectrum of the reference data, different wall temperature, and different Mach number. At the lowest value of $\sqrt{\overline{u'^2_\infty}}/U_e \approx 2 \times 10^{-4}$, transition-point behavior on wind-tunnel models tends to approach the lower levels indicated for cones in free flight (ref. 46) and aeroballistic range cones (ref. 1) that have presumably negligible influence due to disturbance level.

Variations in $R_{1,tr}$ for the flight (ref. 46) and range (ref. 1) data are indicative of unit Reynolds number and Mach number effects and are not plotted at a particular disturbance level but merely serve as a comparison for the tunnel data. Actual disturbance levels representative of the range and flight data are expected to be at least 1 or 2 orders of magnitude lower than indicated in figure 4. The trend of the transition results shown in figure 4 (an increase in $R_{1,tr}$ with a decrease in disturbance level) is in agreement with that expected from Mack's stability theory (refs. 48 to 50) for first mode instability at $0 \leq M_\infty \leq 4$ (increasing $R_{1,tr}$ with increasing Mach number for low disturbance level). The data of figure 4 do not indicate a significant effect of model geometry on the noise-transition results, but indicate only the influence of the free-stream disturbance level divided by edge conditions and the inherent characteristic energy spectra of a given reference wind tunnel that are implicitly included.

Figure 5 shows the different variations of $R_{1,tr}$ with a nondimensionalized free-stream disturbance level for sharp cones and flat plates at supersonic/hypersonic speeds ($4 \leq M_\infty \leq 23$) where the results of references 48 to 50 may be indicative of the trend. It is discussed in reference 4 and shown in reference 45 that transition Reynolds numbers on cones and cylinders may differ by a varying factor for $3 < M_e < 10$ at about the same unit Reynolds number. For $M_e \approx 3$, the established factor varies from 3 to 1.6; for $5 \leq M_e \leq 7$, it varies from 1.4 to 1.1; and for $M_e \approx 8$, no definite conclusion was reached as to the cause of these observed differences. The results in figure 4 ($0 \leq M_\infty \leq 4$) show no large differences in $R_{1,tr}$ between axisymmetric and planar bodies. Transition values shown in figure 5 ($4 \leq M_\infty \leq 23$) over a range of unit Reynolds numbers for cones and flat plates differ in level by about the same factors as might be expected from the results of reference 45. Boundary-layer stability or $R_{1,tr}$ increases with decreasing disturbance level (fig. 5) in a trend similar to that for $M_\infty < 4$ (fig. 4) and similar models, but it reaches significantly higher values for $M_e > 10$. In particular, the sharp-cone results (fig. 5) at the lowest disturbance levels tend to approach the $R_{1,tr}$ values

obtained for flight data at $M_e \approx 15$. This trend in the wind-tunnel transition data is not too surprising since references 49 and 50 show that, for mode 2 instabilities and constant Reynolds number, the maximum spatial amplification rate changes by about the same order of magnitude as do the transition results in figure 5 over the Mach number range $4 \leqq M_\infty \leqq 20$. A comparison of the experimentally observed, most unstable frequencies (refs. 51 and 52) with the second-mode theoretical results (refs. 49 and 50) for sharp cones at hypersonic speeds has served to identify the estimation of transition trends at high speeds and, to a certain extent, the periodic waves.

It should be recalled that the radiated free-stream pressure fluctuations $\sqrt{p_\infty'^2}/p_\infty$ increase with increasing M_∞ and reach very high levels (fig. 1(a)). The highest values of $R_{1,tr}$ shown in figure 5 were obtained on models in wind tunnels and correspond to high Mach numbers ($M_\infty \approx 20$), but also to high values of absolute disturbance level. This fact provokes questions concerning the effects of absolute disturbance level on transition; both disturbance level and transition are known to vary with unit Reynolds number and from tunnel to tunnel. However, when $R_{1,tr}$ is correlated with the free-stream disturbance level divided by local dynamic pressure, the data tend to collapse and agree with the individual data fairings (fig. 5) to within about 20 percent for cones and flat plates. Accounting for both free-stream disturbance level and local conditions is certainly not the only function controlling transition but does serve as a significant improvement over previous attempts (refs. 7 and 16) to correlate noise-transition data for a large number of tunnels. It may be that the ability of large-amplitude external disturbances to induce transition is reduced at local conditions that correspond to high Mach number flow. In all probability, the amplified critical frequencies are more important than disturbance level. The results in figures 4 and 5 indicate that transition measurements on models could more closely simulate those in flight if ground test facilities were properly designed to reduce flow noise to approximately those levels and scales expected in flight (ref. 43). It would be highly desirable to be able to vary both disturbance level and energy spectra in such quiescent tunnels. An effort has been made toward the development of a Mach 5 pilot quiet tunnel at the Langley Research Center (refs. 2 and 24) that can be used to investigate the influence of free-stream disturbance level on transition.

CONCLUDING REMARKS

A significant quantity of available data has been compiled and an attempt has been made to evaluate the effects of wind-tunnel disturbance levels on boundary-layer stability and transition on test models.

In general, wind-tunnel root-mean-square disturbance levels divided by free-stream static pressure can be expected to increase with increasing free-stream Mach number ($1.5 \leqq M_\infty \leqq 10$) at the same unit Reynolds number up to low hypersonic Mach numbers and can be expected to decrease at very high Mach numbers ($M \gtrapprox 20$).

The stability of a laminar boundary layer and the subsequent onset of transition for simple axisymmetric and planar surfaces are influenced both by free-

stream disturbance level and local conditions for a wide range of test conditions. The beginning of transition on these surfaces has been shown to collapse along a single curve when correlated with the nondimensional free-stream disturbance level based on local dynamic pressure. The general trend for transition that is expected from linear stability theory at relatively low amplification and hypersonic speeds supports these results. The present results are considered a significant improvement over previous attempts to correlate noise-transition results. Apparently, for sufficiently low disturbance levels in tunnels, transition results that approach corresponding measured values in flight without disturbance effects can be obtained on simple shapes. On the other hand, very high noise levels in tunnels probably dominate transition for any given shape.

Langley Research Center
National Aeronautics and Space Administration
Hampton, VA 23665
February 22, 1978

REFERENCES

1. Potter, J. Leith: Boundary-Layer Transition on Supersonic Cones in an Aeroballastic Range. AIAA J., vol. 13, no. 3, Mar. 1975, pp. 270-277.

2. Beckwith, I. E.: Development of a High Reynolds Number Quiet Tunnel for Transition Research. AIAA J., vol. 13, no. 3, Mar. 1975, pp. 300-306.

3. Reshotko, Eli: Stability Theory as a Guide to the Evaluation of Transition Data. AIAA J., vol. 7, no. 6, June 1969, pp. 1086-1091.

4. Morkovin, Mark V.: Critical Evaluation of Transition From Laminar to Turbulent Shear Layers With Emphasis on Hypersonically Traveling Bodies. AFFDL-TR-68-149, U.S. Air Force, Mar. 1969. (Available from DDC as AD 686 178.)

5. Morkovin, Mark V.: Instability Transition to Turbulence and Predictability. IIT Paper presented at the Fluid Dynamics Panel Symposium (Lyngby, Denmark), May 2-4, 1977.

6. Stainback, P. C.; Fischer, M. C.; and Wagner, R. D.: Effects of Wind-Tunnel Disturbances on Hypersonic Boundary-Layer Transition. Pts. I and II. AIAA Paper No. 72-181, Jan. 1972.

7. Stainback, P. Calvin: Hypersonic Boundary-Layer Transition in the Presence of Wind-Tunnel Noise. AIAA J., vol. 9, no. 12, Dec. 1971, pp. 2475-2476.

8. Stainback, P. Calvin; Wagner, Richard D.; Owen, F. Kevin; and Horstman, Clifford C.: Experimental Studies of Hypersonic Boundary-Layer Transition and Effects of Wind-Tunnel Disturbances. NASA TN D-7453, 1974.

9. Fischer, M. C.; and Wagner, R. D.: Transition and Hot-Wire Measurements in Hypersonic Helium Flow. AIAA J., vol. 10, no. 10, Oct. 1972, pp. 1326-1332.

10. Laufer, John: Factors Affecting Transition Reynolds Numbers on Models in Supersonic Wind Tunnels. J. Aeronaut. Sci., vol. 21, no. 7, July 1954, pp. 497-498.

11. Laufer, John; and Marte, Jack E.: Results and a Critical Discussion of Transition-Reynolds-Number Measurements on Insulated Cones and Flat Plates in Supersonic Wind Tunnels. Report No. 20-96 (Contract No. DA-04-495-Ord 18), Jet Propul. Lab., California Inst. Technol., Nov. 30, 1955.

12. Wagner, R. D., Jr.; Maddalon, D. V.; and Weinstein, L. M.: Influence of Measured Freestream Disturbances on Hypersonic Boundary-Layer Transition. AIAA J., vol. 8, no. 9, Sept. 1970, pp. 1664-1670.

13. Pate, S. R.; and Schueler, C. J.: Radiated Aerodynamic Noise Effects on Boundary-Layer Transition in Supersonic and Hypersonic Wind Tunnels. AIAA J., vol. 7, no. 3, Mar. 1969, pp. 450-457.

14. Laufer, John: Some Statistical Properties of the Pressure Field Radiated by a Turbulent Boundary Layer. Phys. Fluids, vol. 7, no. 8, Aug. 1964, pp. 1191-1197.

15. Laderman, A. J.: Review of Wind-Tunnel Freestream Pressure Fluctuations. AIAA J., vol. 15, no. 4, Apr. 1977, pp. 605-608.

16. Bergstrom, E. R.; and Raghunathan, S.: Aerodynamic Noise and Boundary-Layer Transition Measurements in Supersonic Test Facilities. AIAA J., vol. 10, no. 11, Nov. 1972, pp. 1531-1532.

17. Dougherty, N. S., Jr.: Correlation of Transition Reynolds Number With Aerodynamic Noise Levels in a Wind Tunnel at Mach Numbers 2.0-3.0. AIAA J., vol. 13, no. 12, Dec. 1975, pp. 1670-1671.

18. Dougherty, N. S., Jr.: Prepared Comment on the Cone Transition Reynolds Number Data Correlation Study. Flight/Ground Testing Facilities Correlation, AGARD-CP-187, 1976, pp. 3A-1 - 3A-7.

19. Stainback, P. C.; and Rainey, R. A.: Correlation of Freestream Pressure Disturbances in Supersonic Wind Tunnels. AIAA J., vol. 14, no. 2, Feb. 1976, pp. 286-288.

20. Whitfield, Jack D.; and Dougherty, N. Sam, Jr.: A Survey of Transition Research at AEDC. Laminar-Turbulent Transition, AGARD-CPP-224, 1977, pp. 25-1 - 25-20.

21. Harvey, William D.; and Hunter, William W., Jr.: Experimental Study of a Free Turbulent Shear Flow at Mach 19 With Electron-Beam and Conventional Probes. NASA TN D-7981, 1975.

22. Harvey, William D.; Bushnell, Dennis M.; and Beckwith, Ivan E.: Fluctuating Properties of Turbulent Boundary Layers for Mach Numbers up to 9. NASA TN D-5496, 1969.

23. Kemp, Joseph H.; and Owen, F. Kevin: Experimental Study of Nozzle Wall Boundary Layers at Mach Numbers 20 to 47. NASA TN D-6965, 1972.

24. Beckwith, I. E.; Anders, J. B.; Stainback, P. C.; Harvey, W. D.; and Srokowski, A. J.: Progress in the Development of a Mach 5 Quiet Tunnel. Laminar-Turbulent Transition, AGARD-CPP-224, 1977, pp. 28-1 - 28-14.

25. Laderman, A. J.; and Demetriades, A.: Mean and Fluctuating Flow Measurements in the Hypersonic Boundary Layer Over a Cooled Wall. J. Fluid Mech., vol. 63, pt. 1, Mar. 18, 1974, pp. 121-144.

26. Donaldson, J. C.; and Wallace, J. P.: Flow Fluctuation Measurements at Mach Number 4 in the Test Section of the 12-Inch Supersonic Tunnel. AEDC-TR-71-143, U.S. Air Force, Aug. 1971. (Available from DDC as AD 728 630.)

27. Dougherty, N. S., Jr.; and Steinle, Frank W., Jr.: Transition Reynolds Number Comparisons in Several Major Transonic Tunnels. AIAA Paper No. 74627, July 1974.

28. Dodds, Jules B., Jr.; and Hanley, Richard D.: Evaluation of Transonic and Supersonic Wind-Tunnel Background Noise and Effects of Surface Pressure Fluctuation Measurements. AIAA Paper No. 72-1004, Sept. 1972.

29. Burnage, H.; and Gaviglio, J.: Some Measurements in the Transitional Supersonic Wake of a Transverse Circular Cylinder With Emphasis on the Effect of External Noise. Laminar-Turbulent Transition, AGARD-CPP-224, 1977, pp. 15-1 - 15-11.

30. Matting, Fred W.; Chapman, Dean R.; Nyholm, Jack R.; and Thomas, Andrew G.: Turbulent Skin Friction at High Mach Numbers and Reynolds Numbers in Air and Helium. NASA TR R-82, 1961.

31. Lilley, G. M.: Wall Pressure Fluctuations Under Turbulent Boundary Layers at Subsonic and Supersonic Speeds. CoA Note 140, College of Aeronaut., Cranfield (England), Mar. 1963.

32. Kistler, A. L.; and Chen, W. S.: The Fluctuating Pressure Field in a Supersonic Turbulent Boundary Layer. J. Fluid Mech., vol. 16, pt. 1, May 1963, pp. 41-64.

33. Bull, M. K.: Properties of the Fluctuating Wall Pressure Field of a Turbulent Boundary Layer. AGARD Rep. 455, Apr. 1963.

34. Willmarth, W. W.; and Roos, F. W.: Resolution and Structure of the Wall Pressure Field Beneath a Turbulent Boundary Layer. J. Fluid Mech., vol. 22, pt. 1, May 1965, pp. 81-94.

35. Harrison, Mark: Pressure Fluctuations on the Wall Adjacent to a Turbulent Boundary Layer. Rep. 1260, David Taylor Model Basin, Navy Dept., Dec. 1958.

36. Fischer, M. C.; Maddalon, D. V.; Weinstein, L. M.; and Wagner, R. D., Jr.: Boundary-Layer Pitot and Hot-Wire Surveys at $M_\infty \approx 20$. AIAA Paper 70746, June-July 1970.

37. Belcher, Peter M.: Predictions of Boundary-Layer-Turbulence Spectra and Correlations for Supersonic Flight. 5^{e} Congrès International d'Acoustique, vol. I^{b}, Daniel E. Commins, ed., Congr. Int. Acoustique, 1965, pp. [L54] 1-4.

38. Lowson, M. V.: Prediction of Boundary Layer Pressure Fluctuations. AFFDL-TR-67-167, U.S. Air Force, Apr. 1968. (Available from DDC as AD 832 715.)

39. Speaker, W. V.; and Ailman, C. M.: Spectra and Space-Time Correlations of the Fluctuating Pressures at a Wall Beneath a Supersonic Turbulent Boundary Layer Perturbed by Steps and Shock Waves. NASA CR-486, 1966.

40. Raman, K. R.: Surface Pressure Fluctuations in Hypersonic Turbulent Boundary Layers. NASA CR-2386, 1974.

41. Chen, William S.: Measurements of Aerodynamic Noise on a Flat Plate in Supersonic Flow. Aeronaut. Eng. Thesis, California Inst. Technol., 1961.

42. Maestrello, L.; Monteith. J. H., Manning, J. C.; and Smith, D. L.: Measured Response of a Complex Structure to Supersonic Turbulent Boundary Layers. AIAA Paper No. 76-83, Jan. 1976.

43. MacCready, Paul B., Jr.: Turbulence Measurements by Sailplane. J. Geophys. Res., vol. 67, no. 3, Mar. 1962, pp. 1041-1050.

44. Pfenninger, Werner; and Reed, Verlin D.: Laminar-Flow Research and Experiments. Astronaut. & Aeronaut., July 1966, pp. 44-50.

45. Potter, J. Leith; and Whitfield, Jack D.: Boundary-Layer Transition Under Hypersonic Conditions. AEDC-TR-65-99, U.S. Air Force, May 1965.

46. Wright, Robert L.; and Zoby, Ernest V.: Flight Boundary Layer Transition Measurements on a Slender Cone at Mach 20. AIAA Paper 77-719, June 1977.

47. Pate, S. R.: Comparison of NASA Helium Tunnel Transition Data With Noise-Transition Correlation. AIAA J., vol. 12, no. 11, Nov. 1974, p. 1615.

48. Mack, Leslie M.: Linear Stability Theory and the Problem of Supersonic Boundary-Layer Transition. AIAA J., vol. 13, no. 3, Mar. 1975, pp. 278-289.

49. Mack, Leslie M.: A Numerical Method for the Prediction of High-Speed Boundary-Layer Transition Using Linear Theory. Aerodynamic Analysis Requiring Advanced Computers - Part I, NASA SP-347, 1975, pp. 101-120.

50. Mack, Leslie M.: On the Application of Linear Stability Theory to the Problem of Supersonic Boundary-Layer Transition. AIAA Paper No. 74-134, Jan.-Feb. 1974.

51. Demetriades, Anthony: Hypersonic Viscous Flow Over a Slender Cone. Part III: Laminar Instability and Transition. AIAA Paper No. 74-535, June 1974.

52. Kendall, J. M.: Wind Tunnel Experiments Relating to Supersonic and Hypersonic Boundary-Layer Transition. AIAA J., vol. 13, no. 3, Mar. 1975, pp. 290-299.

53. Pate, S. R.: Measurements and Correlations of Transition Reynolds Numbers on Sharp Slender Cones at High Speeds. AIAA J., vol. 9, no. 6, June 1971, pp. 1082-1090.

54. Schubauer, G. B.; and Skramstad, H. K.: Laminar-Boundary-Layer Oscillations and Transition on a Flat Plate. NACA Rep. 909, 1948.

55. Wells, C. Sinclair, Jr.: Effects of Freestream Turbulence on Boundary-Layer Transition. AIAA J., vol. 5, no. 1, Jan. 1967, pp. 172-174.

56. Boltz, Frederick W.; Kenyon, George C.; and Allen, Clyde O.: The Boundary-Layer Transition Characteristics of Two Bodies of Revolution, a Flat Plate, and an Unswept Wing in a Low-Turbulence Wind Tunnel. NASA TN D-309, 1960.

57. Dryden, Hugh L.: Air Flow in the Boundary Layer Near a Plate. NACA Rep. 562, 1936.

58. Hall, A. A.; and Hislop, G. S.: Experiments on the Transition of the Laminar Boundary Layer on a Flat Plate. R. & M. No. 1843, British A.R.C., 1938.

59. Spangler, J. G.; and Wells, C. S., Jr.: Effects of Freestream Disturbances on Boundary-Layer Transition. AIAA J., vol. 6, no. 3, Mar. 1968, pp. 543-545.

60. Morkovin, Mark V.: On Transition Experiments at Moderate Supersonic Speeds. J. Aeronaut. Sci., vol. 24, no. 7, July 1957, pp. 480-486.

61. Coles, Donald: Measurements of Turbulent Friction on a Smooth Flat Plate in Supersonic Flow. J. Aeronaut. Sci., vol. 21, no. 7, July 1954, pp. 433-448.

DEFINITIONS OF FACILITY ABBREVIATIONS USED IN TABLES I TO III

ARC 11' TWT	Ames 11-Foot Transonic Wind Tunnel
ARC 14' TWT	Ames 14-Foot Transonic Wind Tunnel
ARC M-50	Ames M-50 helium tunnel
ARC 9 × 7' SWT	Ames 9- by 7-Foot Supersonic Wind Tunnel
ARC 3.5' HWT	Ames 3.5-Foot Hypersonic Wind Tunnel
ARC 12' PWT	Ames 12-Foot Pressure Wind Tunnel
AWT(4T)	AEDC Aerodynamic Wind Tunnel (4T)
CAL 48" HST	Calspan 48-inch leg of the hypersonic shock tunnel (formerly Cornell Aeronautical Laboratory 48-inch hypersonic shock tunnel)
CSWT	The Johns Hopkins University continuous supersonic wind tunnel
GDFTA	AEDC von Kármán Gas Dynamics Facility Tunnel A
GDFTB	AEDC von Kármán Gas Dynamics Facility Tunnel B
GDFTD	AEDC von Kármán Gas Dynamics Facility Tunnel D
IMST(S7) or (S8)	low turbulence wind tunnel of the Institut de Mécanique Stati.tique de la Turbulence (asymmetric nozzle or symmetric nozzle)
JPL 20" SWT	JPL 20-Inch Supersonic Wind Tunnel
JPL 21" HWT	JPL 21-Inch Hypersonic Wind Tunnel
LaRC 4' SPT	Langley 4-foot supersonic pressure tunnel
LaRC HeT	1.52-meter (60-inch) diameter test section of the Langley high Reynolds number helium tunnel
LaRC HRNT	Mach 6 high Reynolds number tunnel at the Langley Research Center
LaRC HNT	Langley hypersonic nitrogen tunnel
LaRC M5	Mach 5 pilot quiet tunnel at the Langley Research Center
LaRC 16'TT	Langley 16-foot transonic tunnel

LaRC 20"	Langley 20-inch Mach 6 tunnel
LaRC 22"	22-inch aerodynamic leg of Langley hypersonic helium tunnel facility
LaRC UPWT(1) or (2)	Langley Unitary Plan wind tunnel (test section 1 or 2)
LaRC VD	Langley Mach 8 variable-density hypersonic tunnel
LTV BLC	LTV Research Center Boundary Layer Channel
LUTGT	Loughborough University of Technology Gun Tunnel
NBS $4\frac{1}{2}$' WT	NBS $4\frac{1}{2}$-foot wind tunnel
PWT(16S)	AEDC Propulsion Wind Tunnel (16S)
RANGE K	AEDC Range K

TABLE I.- DATA SOURCE FOR FIGURE 1

$[M_{\infty,air} = 1.291 M_{\infty,He}]$

Symbol	M_∞	Type of measurement	t_w/t_t	γ	R_∞ per meter	R_∞ per inch	Facility	Source
○	1.6 to 5	Hot wire	1.0	1.4	3.54×10^6 13.39	0.09×10^6 .34	JPL 20" SWT	Laufer (ref. 14)
△	7.32	Hot wire	0.47	1.4	15.35×10^6 11.46	0.39×10^6 .291	ARC 3.5 HWT	Stainback, Wagner, Owen, and Horstman (ref. 8)
◁	8.62 8.25 8.82 8.89	Acoustic, rms pitot[a]	0.39 .090 .146 .180	1.4	2.62×10^6 5.00 6.02 6.97	0.092×10^6 .127 .153 .177	CAL 48" HST	Harvey, Bushnell, and Beckwith (ref. 22)
⊕	18.72 19.76	rms density[b]	0.183 .180	1.4	1.66×10^6 32.8	0.0422×10^6 .833	LaRC HNT	Harvey and Hunter (ref. 21)
◇	49.2	Hot wire	0.574	1.67	4.22×10^6	0.107×10^6	ARC M-50	Kemp and Owen (ref. 23)
[c]◺	5 4.05 3.78 3.47	Hot wire	≈0.85	1.4	15.0×10^6	0.381×10^6	LaRC M5	Beckwith, Anders, Stainback, Harvey, and Srokowski (ref. 24)
[c]◪	2.27 2.47 2.68	Hot wire	≈0.85	1.4	$(11.7 \text{ to } 51.2) \times 10^6$ $(21.2 \text{ to } 50.5)$ $(19.7 \text{ to } 48.0)$	$(0.297 \text{ to } 1.3) \times 10^6$ $(0.538 \text{ to } 1.28)$ $(0.50 \text{ to } 1.22)$	LaRC M5	Unpublished
∪	6.95	Hot wire	0.40	1.4	10.51×10^6 12.05 14.41 16.26	0.267×10^6 .306 .366 .413	LUTGT	Bergstrom and Raghunathan (ref. 16)
◿	23.24 25.95 28.14	Hot wire	1.0	1.67	7.09×10^6 16.93 30.71	0.180×10^6 .430 .780	LaRC 22"	Fischer and Wagner (ref. 9)

[a]Converted rms pitot to rms static pressure.
[b]Converted rms density to rms static pressure.
[c]M_∞ at acoustic origin.

TABLE I.- Continued

Symbol	M_∞	Type of measurement	t_w/t_t	γ	R_∞ per meter	R_∞ per inch	Facility	Source
	21.62 23.24	Hot wire	1.0	1.67	7.87×10^6 39.37	0.20×10^6 1.0	LaRC HeT	Fischer and Wagner (ref. 9)
	8	Hot wire	0.75	1.4	5.51×10^6 8.66	0.14×10^6 .22	GDFTB	Laderman (ref. 15)
	9.4	Hot wire	0.40	1.4	5.12×10^6	0.13×10^6	JPL 21" HWT	Laderman and Demetriades (ref. 25)
	6	Hot wire	0.75	1.4	7.48×10^6 17.32	0.19×10^6 .44	GDFTB	Laderman (ref. 15)
	4	Hot wire	1.0	1.4	1.97×10^6 9.45	0.05×10^6 .24	GDFTD	Donaldson and Wallace (ref. 26)
	1.6 1.6 2.0 2.0	Acoustic, 10° cone	1.0	1.4	3.28×10^6 13.11 3.28 16.42	0.0833×10^6 .333 .0833 .417	LaRC 4' SPT	Dougherty (ref. 18)
	1.6 2.0 2.0 2.86 2.86	Acoustic, 10° cone	1.0	1.4	6.54×10^6 3.28 16.42 3.28 6.54	0.166×10^6 .0833 .417 .0833 .166	LaRC UPWT(1) LaRC UPWT(1) LaRC UPWT(1) LaRC UPWT(1) LaRC UPWT(2)	Dougherty (ref. 18)
	6	Acoustic, 10° cone	0.62	1.4	24.80×10^6 59.06	0.63×10^6 1.5	LaRC HRNT	Stainback (ref. 7)
	6	Acoustic, 10° cone	0.62	1.4	9.45×10^6 32.68	0.24×10^6 .83	LaRC 20"	Stainback (ref. 7)
	8	Acoustic, 16° cone	0.40	1.4	3.15×10^6 27.17	0.08×10^6 .69	LaRC VD	Stainback (ref. 7)
	3 3 5 5	Acoustic, flat plate	1.0	1.4	1.97×10^6 27.56 5.91 27.56	0.05×10^6 .70 .15 .70	GDFTA	Pate and Schueler (ref. 13)

TABLE I.- Continued

Symbol	M_∞	Type of measurement	t_w/t_t	γ	R_∞ per meter	R_∞ per inch	Facility	Source
△	6	Acoustic, 10° cone	0.62	1.4	15.75×10^6 62.99	0.4×10^6 1.6	LaRC HRNT	Beckwith (ref. 2)
○	25.3 25.8 26.9 28.2 29.3	Acoustic, 16° cone	1.0	1.67	13.39×10^6 9.06 23.62 19.29 48.03	$0.[illegible] \times 10^6$ .23 .60 .49 1.22	LaRC 22"	Stainback (ref. 7)
□	2 2 2.5 2.5 3 3	Acoustic, 10° cone	1.0	1.4	4.92×10^6 3.94 4.92 2.76 3.94 1.97	0.125×10^6 .10 .125 .07 .10 .05	PWT(16S)	Dougherty (ref. 17)
●	0.4 .6 .8 1.0 1.2 1.3 .3	Acoustic, 10° cone	1.0	1.4	$(6.57$ to $9.84) \times 10^6$ (6.57 to 13.11) (6.57 to 13.11) (6.57 to 13.11) (9.84 to 13.11) (6.57 to 13.11) (6.57 to 9.84)	$(0.167$ to $0.25) \times 10^6$ (0.167 to 0.333) (0.167 to 0.333) (0.167 to 0.333) (0.25 to 0.333) (0.167 to 0.333) (0.167 to 0.25)	AWT(4T) (porous walls)	Dougherty and Steinle (ref. 27)
◆	0.4 .8	Acoustic, 10° cone	1.0	1.4	8.50×10^6 13.11	0.216×10^6 .333	ARC 14' TWT (slots)	Dougherty and Steinle (ref. 27)
◇	0.6 .8 .9 1.0 1.2 1.4	Acoustic, flat plate	1.0	1.4	5.577×10^6 5.577 5.577 5.577 5.577 30.84	0.142×10^6 .142 .142 .142 .142 .783	ARC 11" TWT	Dodds and Hanley (ref. 28)

TABLE I.- Concluded

Symbol	M_∞	Type of measurement	t_w/t_t	γ	R_∞ per meter	R_∞ per inch	Facility	Source
◹	1.6 1.8 2.0 2.2 2.6	Acoustic, flat plate	1.0	1.4	4.92×10^6 4.92 4.92 4.92 21.33	0.125×10^6 .125 .125 .125 .542	ARC 9 × 7' SWT	Dodds and Hanley (ref. 28)
▲	0.3 1.3	Acoustic, 10° cone	1.0	1.4	4.25×10^6 12.80	0.108×10^6 .325	LaRC 16' TT (slots)	Dougherty and Steinle (ref. 27)
■	0.2 .3 .4 .6 .7 1.0 1.4 1.6	Acoustic, 10° cone	1.0	1.4	6.57×10^6 6.57 6.57 (6.57 to 13.11) (6.57 to 16.42) (6.57 to 16.42) (6.57 to 16.42) 6.57	0.167×10^6 .167 .167 (0.167 to 0.333) (0.167 to 0.417) (0.167 to 0.417) (0.167 to 0.417) .167	LaRC 16' TT (slots)	Dougherty and Steinle (ref. 27)
◺	0.2 .3 .4 .6 .7 .8 .9	Acoustic, flat plate	1.0	1.4	20.31×10^6 29.53 17.24 9.84 8.19 5.91 4.92	0.516×10^6 .75 .438 .25 .208 .150 .125	ARC 12' PWT	Dodds and Hanley (ref. 28)
◇	2.3	Hot wire	≈1.0	1.4			IMST(S7)	Burnage and Gaviglio (ref. 29)
◇	2.3	Hot wire	≈1.0	1.4			IMST(S8)	Burnage and Gaviglio (ref. 29)

TABLE II.- DATA SOURCE FOR FIGURE 2

$[M_{\infty,air} = 1.291 M_{\infty,He}]$

Symbol	M_∞	Type of measurement	Location of measurement	t_w/t_t	γ	Facility	Source
	6.95	Hot wire	Free stream	----	1.4	LUTGT	Bergstrom and Raghunathan (ref. 16)
	23.4 to 28.1	Hot wire	Free stream	1.0	1.67	LaRC 22"	Stainback, Fischer, and Wagner (ref. 6)
	25.3 to 29.4	Acoustic, 16° cone	Free stream	1.0	1.67	LaRC 22"	Stainback, Fischer, and Wagner (ref. 6)
	4	Hot wire	Free stream	1.0	1.4	GDFTD	Donaldson and Wallace (ref. 26)
	6	Acoustic, 10° cone	Free stream	0.62	1.4	LaRC HRNT	Stainback (ref. 7)
	6	Acoustic, 10° cone	Free stream	0.62	1.4	LaRC 20"	Stainback (ref. 7)
	7.32	Acoustic, 10° cone	Free stream	0.47	1.4	ARC 3.5 HWT	Stainback, Wagner, Owen, and Horstman (ref. 8)
	8	Acoustic, 16° cone	Free stream	0.40	1.4	LaRC VD	Stainback (ref. 7)
	8	Hot wire	Free stream	0.75	1.4	GDFTB	Laderman (ref. 15)
	7.32	Hot wire	Free stream	0.47	1.4	ARC 3.5 HWT	Stainback, Wagner, Owen, and Horstman (ref. 8)
	9.4	Hot wire	Free stream	0.40	1.4	JPL 21" HWT	Laderman and Demetriades (ref. 25)
	21.4 to 23.23	Hot wire	Free stream	1.0	1.67	LaRC HeT	Stainback, Fischer, and Wagner (ref. 6)

TABLE II.- Concluded

Symbol	M_∞	Type of measurement	Location of measurement	t_w/t_t	γ	Facility	Source
●	1.6 to 5	Hot wire	Free stream	1.0	1.4	JPL 20" SWT	Laufer (ref. 14)
□	0.3, 0.5	Acoustic	Wall	1.0	1.4	----------	Bull (ref. 33)
▽	0.3, 0.75	Acoustic	Wall	1.0	1.4	----------	Willmarth and Roos (ref. 34)
D	≈0.15	Acoustic	Wall	1.0	1.4	----------	Harrison (ref. 35)
◻	≈29	Acoustic	Wall	1.0	1.67	LaRC 22"	Fischer, Maddalon, Weinstein, and Wagner (ref. 36)
○	0.5 to 5	Acoustic	Wall	1.0	1.4	JPL 20" SWT	Kistler and Chen (ref. 32)
△	0.95 to 1.9	Acoustic	Wall	----------	Air	Flight	Belcher (ref. 37)
◇	0.35 to 0.78	Acoustic	Wall	1.0	1.4	----------	Lowson (ref. 38)
◻, ◢	8.24 to 8.89	Acoustic	Wall, free stream	0.09 to 0.18	1.4	CAL 48" HST	Harvey, Bushnell, and Beckwith (ref. 22)
◊	1 to 2.25	Acoustic	Wall	1.0	1.4	----------	Speaker and Ailman (ref. 39)
◇	5.2, 7.4, 10.4	Acoustic	Flat plate	0.26 to 0.44	1.4	ARC 3.5 HWT	Raman (ref. 40)
◺	2 to 5	Acoustic	Flat plate	----------	1.4	----------	Chen (ref. 41,
◢	3, 5	Acoustic	Flat plate	1.0	1.4	GDFTA	Pate and Schueler (ref. 13)
◆	49.2	Hot wire	Free stream	0.574	1.67	ARC M-50	Kemp and Owen (ref. 23)
◆	18.72, 19.76	Electron beam	Free stream	0.18	1.4	LaRC HNT	Harvey and Hunter (ref. 21)
∪	1.6, 22	Acoustic	Wall	1.0	1.4	PWT(16S)	Maestrello, Monteith, Manning, and Smith (ref. 42)

TABLE III.- DATA SOURCE FOR FIGURES 3, 4, AND 5

Symbol	M_∞	γ	t_w/t_t	Model	Facility	$R_{1,tr}$ measurement	Free-stream noise measurement	Source
◿	≈21	1.67	1.0	2.87°, 16°, sharp cone	LaRC 22"	Heat transfer	Hot wire	Fischer and Wagner (ref. 9)
◿	≈18	1.67	1.0	1.87°, 5°, 10°, sharp cone	LaRC HeT	Heat transfer	Hot wire	Fischer and Wagner (ref. 9)
⬡	8	1.4	0.75	5° sharp cone	GDFTB	Heat transfer	Hot wire	Demetriades (ref. 51)
◇	7.32	1.4	0.47	16° sharp cone	ARC 3.5 HWT	Heat transfer	Hot wire	Stainback, Fischer, and Wagner (ref. 6)
◇	2.2, 4.75	1.4	1.0	10° sharp cone	JPL 20" SWT	Heat transfer	Hot wire	Kendall (ref. 52)
⌂	2.5, 4.5, 1.8	1.4	1.0	10° sharp cone	JPL 20" SWT	Heat transfer	Hot wire	Laufer (ref. 10)
∪	1.3 to 3.7	1.4	1.0	5° sharp cone	JPL 20" SWT	Heat transfer	Hot wire	Laufer and Marte (ref. 11)
▽	1.6, 2	1.4	≈1.0	10° sharp cone	LaRC 4' SPT	Acoustic	Acoustic	Dougherty (ref. 18)
□	6	1.4	0.62	10° sharp cone	LaRC HRNT	Heat transfer	Acoustic	Stainback (ref. 7)
◇	8	1.4	0.40	16° sharp cone	LaRC VD	Heat transfer	Acoustic	Stainback (ref. 7)
△	6	1.4	0.62	16.75° sharp cone	LaRC 20"	Heat transfer	Acoustic	Stainback (ref. 7)
∩	3, 5	1.4	≈1.0	5° sharp cone	GDFTA	Heat transfer	Acoustic	Pate (ref. 53)
▷	1.6, 2, 2.86	1.4	≈1.0	10° sharp cone	LaRC 4' SPT	Acoustic	Acoustic	Dougherty (ref. 18)
⬡	2.9, 3.5, 4.6	1.4	≈1.0	10° sharp cone	LaRC 4' SPT	Acoustic	Acoustic	Dougherty (ref. 18)
I	2.3, 5	1.4	0.52, 0.19	4°, 10° sharp cone	Range K	Photo	Acoustic	Potter (ref. 1)
○	2.5, 2.75	1.4	≈1.0	10° sharp cone	PWT(16S)	Heat transfer	Acoustic	Dougherty (ref. 18)
◇	0.6, 1.0, 1.3	1.4	≈1.0	10° sharp cone	AWT(4T)	Acoustic	Acoustic	Dougherty (ref. 18)

TABLE III.- Concluded

Symbol	M_∞	γ	t_w/t_t	Model	Facility	$R_{1,tr}$ measurement	Free-stream noise measurement	Source
▼	≈20	Air	0.46 to 1.0	10° sharp cone (Reentry F)	Flight test	Heat transfer	--------	Wright and Zoby (ref. 46)
●	0	1.4	≈1.0	Sharp flat plate	NBS 4½' WT	Heat transfer	Hot wire	Schubauer and Skramstad (ref. 54)
■	0	1.4	≈1.0	Tunnel wall	LTV BLC	Hot wire	Hot wire	Wells (ref. 55)
◆	0	1.4	≈1.0	Sharp flat plate	ARC 12' PWT	Heat transfer	Hot wire	Boltz, Kenyon, and Allen (ref. 56)
▲	0	1.4	≈1.0	Sharp flat plate	----------	Heat transfer	Hot wire	Dryden (ref. 57)
◢	0	1.4	≈1.0	Sharp flat plate	----------	Heat transfer	Hot wire	Hall and Hislop (ref. 58)
◢	0	1.4	≈1.0	Tunnel wall	LTV BLC	Heat transfer	Hot wire	Spangler and Wells (ref. 59)
▱	≈18 to 22	1.67	0.68 to 1.0	Sharp flat plate	LaRC 22"	Heat transfer	Hot wire	Wagner, Maddalon, and Weinstein (ref. 12)
◇	1.76	1.4	1.0	Sharp flat plate	CSWT	Pressure	Hot wire	Morkovin (ref. 60)
◇	2 to 4.55	1.4	1.0	Sharp flat plate	JPL 20" SWT	Heat transfer	Hot wire	Laufer and Marte (ref. 11)
▱	1.97 to 4.5	1.4	1.0	Sharp flat plate	JPL 20" SWT	Pressure	Hot wire	Coles (ref. 61)
▽	3	1.4	1.0	Cylinder	GDFTA	Heat transfer	Acoustic, sharp flat plate	Pate and Schueler (ref. 13)
◁	6.95	1.4	1.0	Sharp flat plate	LUTGT	Heat transfer	Hot wire	Bergstrom and Ragunathan (ref. 16)
▽	≈18	1.67	0.33 to 0.92	Sharp flat plate	LaRC HeT	Heat transfer	Hot wire	Unpublished

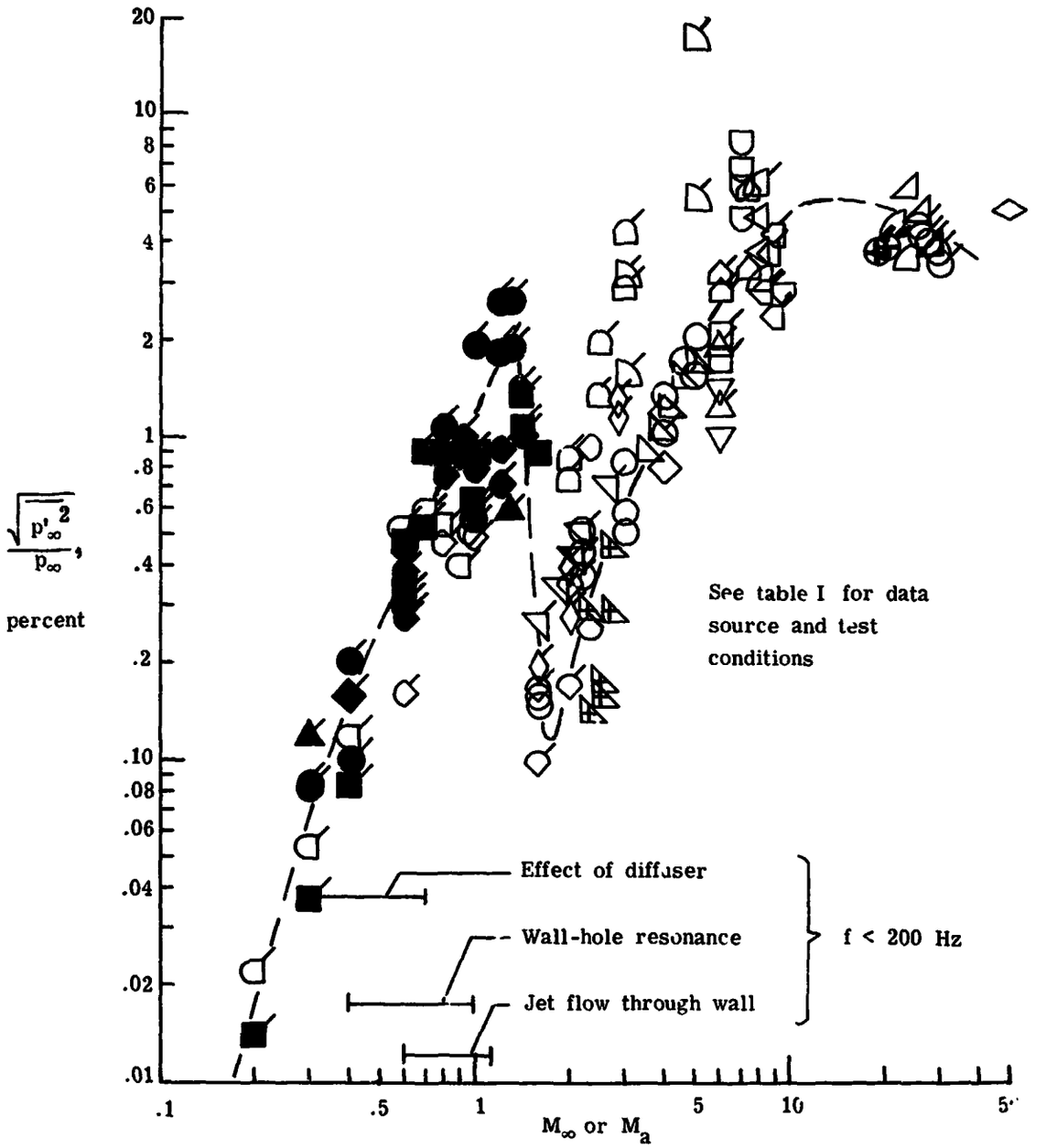

(a) Free-stream rms pressure fluctuations divided by mean static pressure.

Figure 1.- Typical free-stream pressure fluctuations in wind tunnels. $1.65 \times 10^6 \leqq R_\infty/M \leqq 55.2 \times 10^6$; $0.09 \leqq t_w/t_t \leqq 1.0$. Flagged symbols represent data from acoustic measurements; unflagged symbols indicate data from hot-wire measurements; solid symbols indicate data from porous or slotted-wall tunnels; double flag indicates rms density.

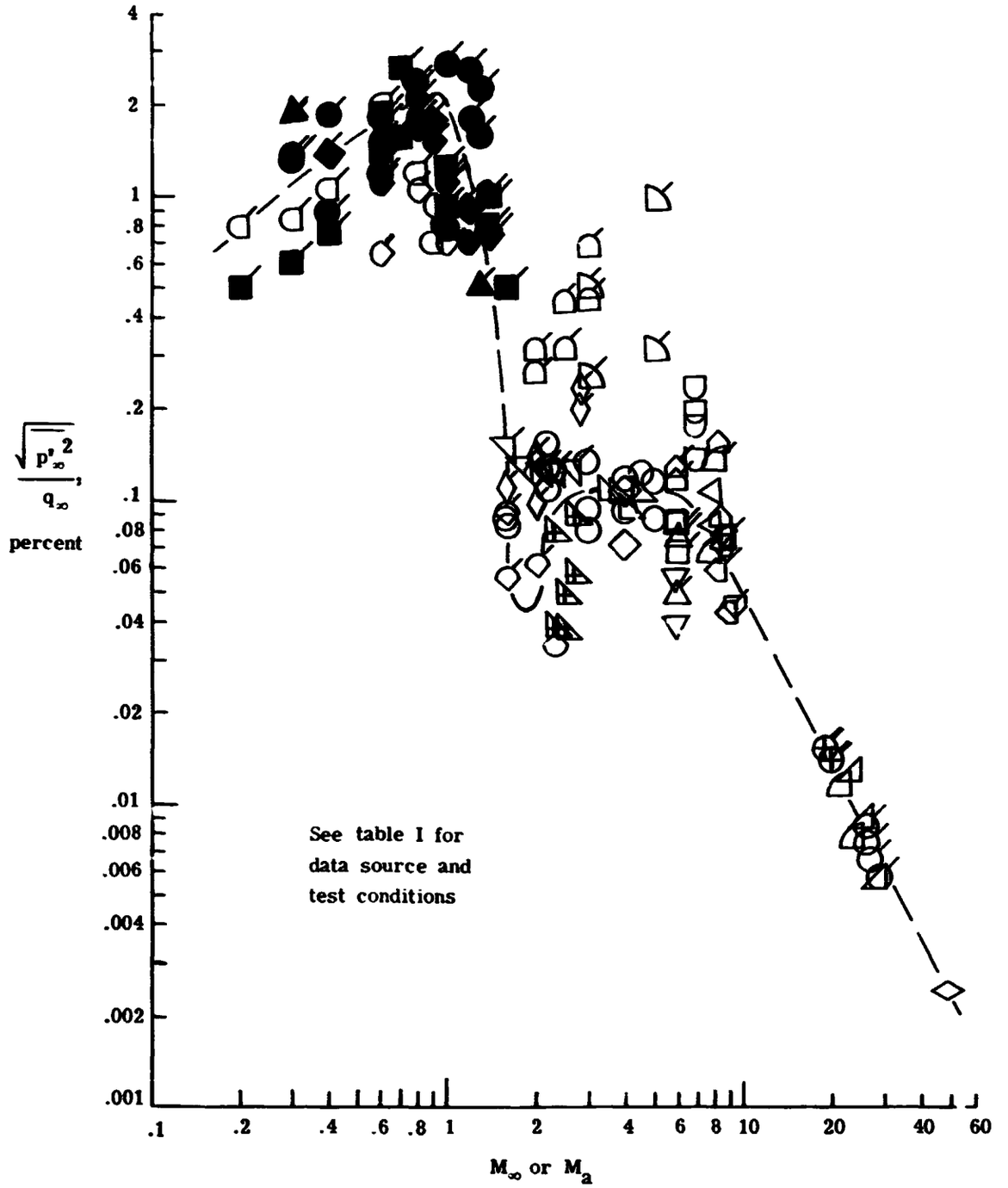

(b) Free-stream rms pressure fluctuations divided by dynamic pressure.

Figure 1.- Concluded.

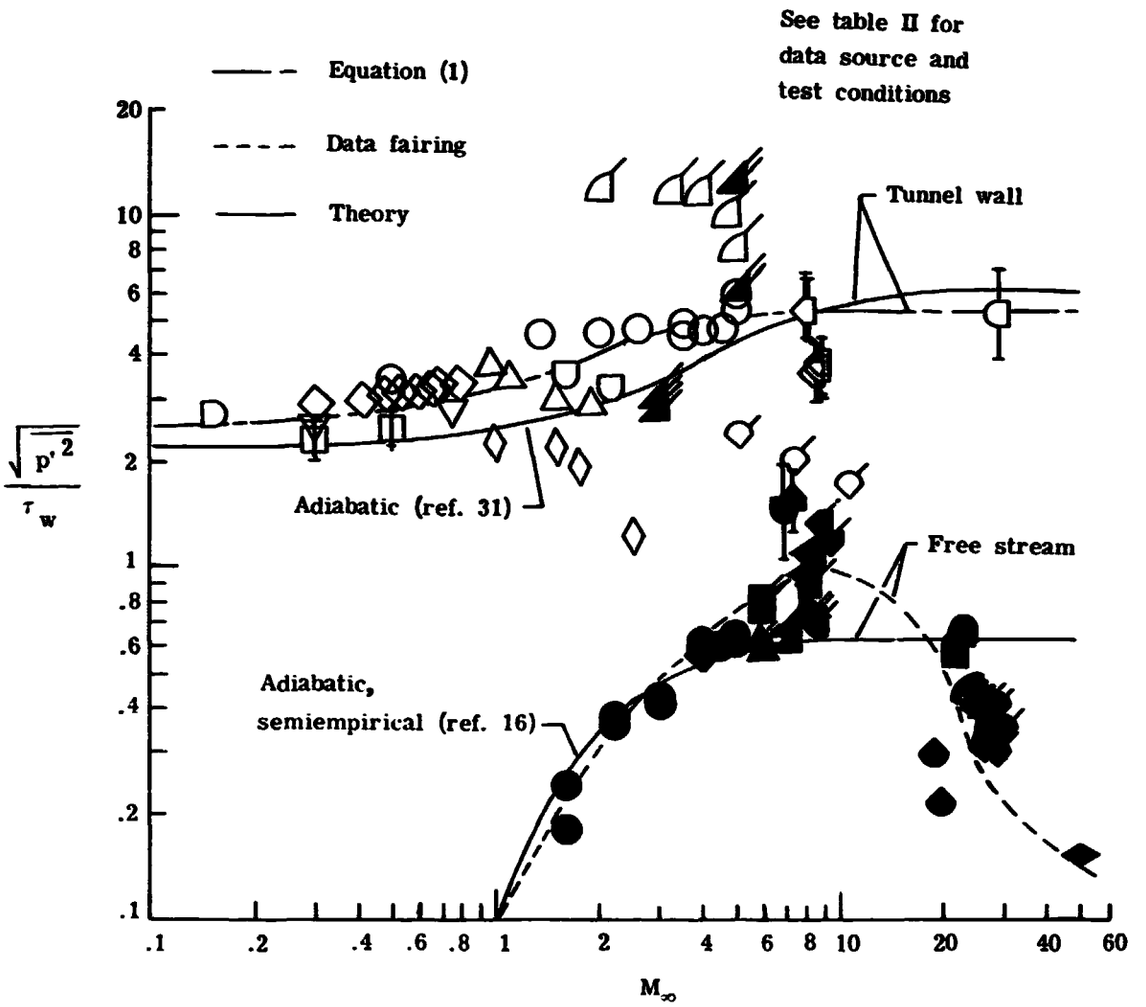

Figure 2.- Comparison of rms wall and free-stream pressure fluctuations. $0.09 \leqq t_w/t_t \leqq 1.0$. Solid symbols indicate free stream; open symbols indicate tunnel wall; flagged symbols indicate acoustic measurements; unflagged symbols indicate hot wire.

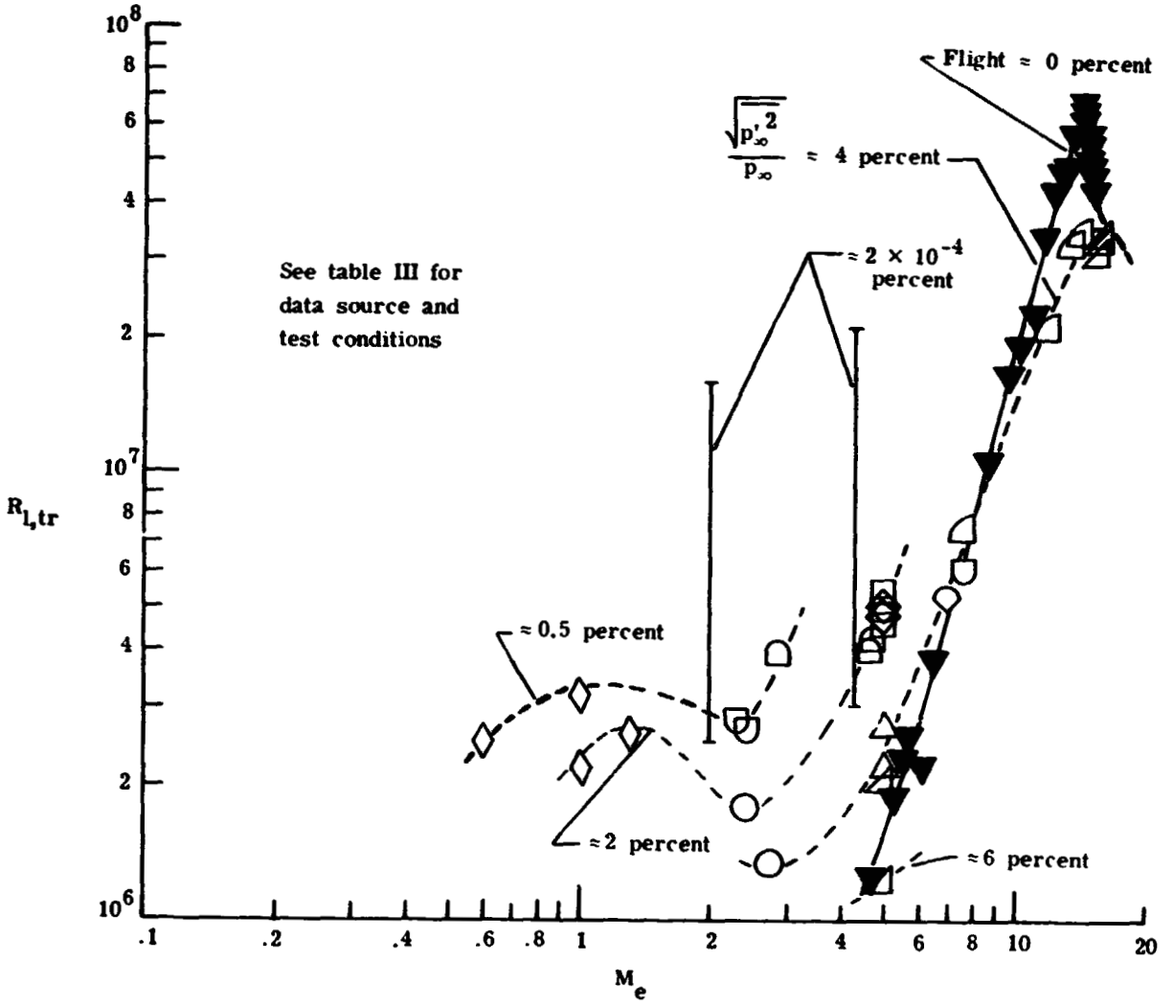

Figure 3.- Transition Reynolds number on sharp cones for several free-stream disturbance levels. $\alpha = 0^o$; $0.1 \leq t_w/t_t \leq 1.0$.

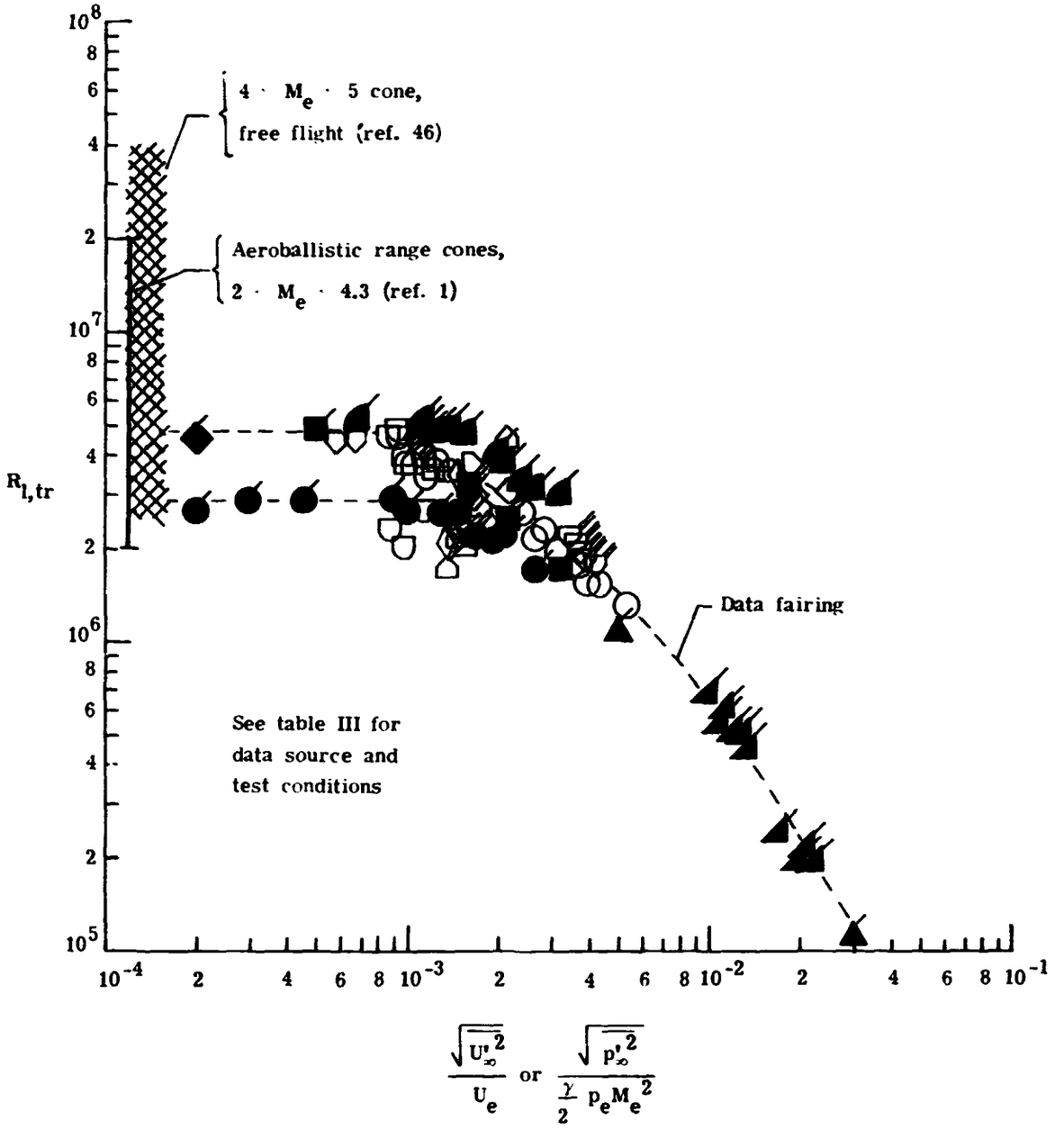

Figure 4.- Influence of free-stream disturbance level on transition for cones, cylinders, and flat plates. $\alpha = 0^o$; $0 \leq M_\infty \leq 4$; $0.4 \leq t_w/t_t \leq 1.0$. Unflagged symbols indicate cones; flagged symbols indicate flat plates or cylinders; solid symbols indicate $\sqrt{\overline{U'^2_\infty}}/U_e$.

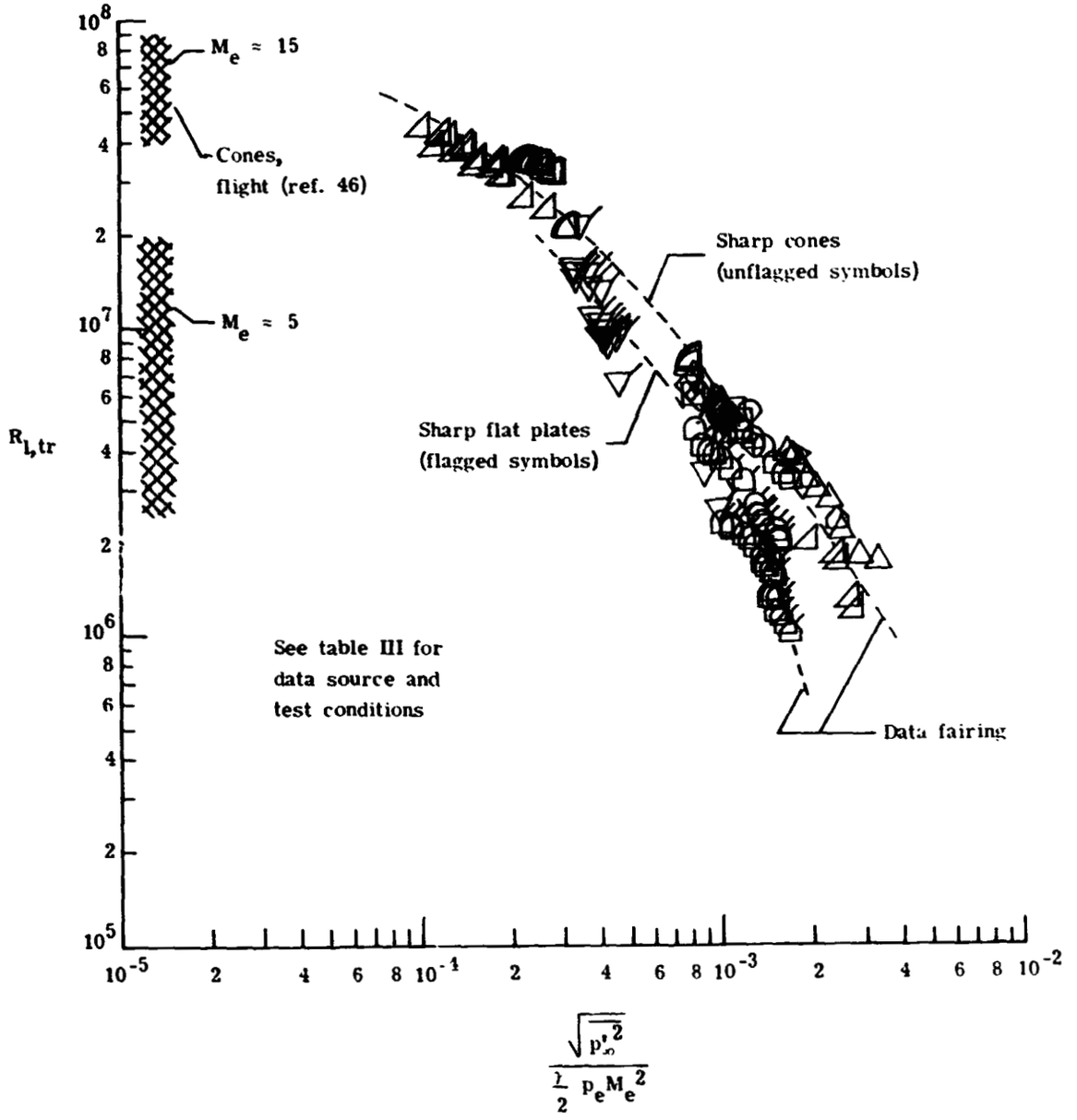

Figure 5.- Influence of free-stream disturbance level on transition for cones and flat plates. $\alpha = 0^o$; $4 \leq M_\infty \leq 23$; $0.3 \leq t_w/t_t \leq 1.0$.

1 Report No.	2 Government Accession No.	3 Recipient's Catalog No
NASA TM-78635		

4 Title and Subtitle	5 Report Date
INFLUENCE OF FREE-STREAM DISTURBANCES ON BOUNDARY-LAYER TRANSITION	April 1978
	6 Performing Organization Code

7 Author(s)	8 Performing Organization Report No
William D. Harvey	L-11905
	10 Work Unit No
9 Performing Organization Name and Address	505-06-41-01
NASA Langley Research Center Hampton, VA 23665	11 Contract or Grant No
	13 Type of Report and Period Covered
12 Sponsoring Agency Name and Address	Technical Memorandum
National Aeronautics and Space Administration Washington, DC 20546	14 Sponsoring Agency Code

15 Supplementary Notes

16 Abstract

Considerable experimental evidence exists which shows that free-stream disturbances (the ratio of root-mean-square pressure fluctuations to mean values) in conventional wind tunnels increase with increasing Mach number at low supersonic to moderate hypersonic speeds. In addition to local conditions, the free-stream disturbance level influences transition behavior on simple test models. Based on this observation, existing noise-transition data obtained in the same test facility have been correlated for a large number of reference sharp cones and flat plates and are shown to collapse along a single curve. This result is a significant improvement over previous attempts to correlate noise-transition data.

17 Key Words (Suggested by Author(s))	18 Distribution Statement
Transition Stream disturbances Noise Boundary layer	Unclassified - Unlimited Subject Category 34

19 Security Classif (of this report)	20 Security Classif (of this page)	21 No of Pages	22 Price*
Unclassified	Unclassified	30	$4.50

* For sale by the National Technical Information Service, Springfield, Virginia 22161